An Integrated Linear Programming Receiver for LDPC Coded MIMO-OFDM Signals

Yong Li, *Member, IEEE,* Lin Wang, *Senior Member, IEEE,* and Zhi Ding, *Fellow, IEEE*

***Abstract*—This work investigates the joint detection and decoding of MIMO-OFDM signals. Traditional receivers either utilize disjoint serial detector and decoder or require turbo message passing between the two functional blocks of detection and decoding. We present a novel approach that can jointly achieve detection and decoding of low density parity check (LDPC) coded multiple-input-multiple-output (MIMO) orthogonal-frequency-division-multiplexing (OFDM) signals as a unified optimization algorithm. Our receiver integrates the MIMO-OFDM signal detection and the decoding of LDPC coded data by formulating a linear programming problem regardless of affine or nonaffine quadrature amplitude modulation (QAM) mapping. The proposed joint MIMO-OFDM detector and decoder achieves substantial performance gain over existing joint detection receivers of comparable computational complexity. Furthermore, the proposed receiver also substantially outperforms the more traditional turbo receiver with only modest cost in complexity.**

***Index Terms*—MIMO-OFDM systems, LDPC codes, linear programming, joint detection.**

I. Introduction

MULTIPLE-input multiple-output (MIMO) transceivers can achieve higher throughput and improved reliability in wireless communications by exploiting spatial diversity in multiple-antenna wireless communications. MIMO signaling has permeated practical state-of-art wireless systems such as IEEE802.11n, LTE-A, and WiMAX by delivering substantial capacity gains. Spatial multiplexing schemes take advantage of increased Shannon capacity that grows linearly with the minimum number of transceiver antennas [1] [2]. Receiver algorithms such as maximum a posteriori probability (MAP) detection, minimum mean square error (MMSE) detection can be utilized for effective MIMO signal detection [7] [8] to achieve the expected diversity gain.

At the same time, the surging need for high speed broadband wireless services has also prompted the widespread adaptation of orthogonal frequency division multiplexing (OFDM) over frequency-selective wireless fading channels as means to mitigate the effect of multipath linear distortions. Among several prominent examples, OFDM and OFDM-base technologies have been incorporated into high profile wireless PHY standards of IEEE802.11(a,g,n) [9] local area network (LAN) standard, IEEE802.16 [10] metropolitan area network (WiMAX) standard, and long term evolution (LTE) [11] cellular standard. OFDM, through a linear IFFT precoder at the transmitter plus cyclic prefix and a corresponding FFT at the receiver, converts a frequency-selective channel into parallel orthogonal and flat subchannels. These orthogonal subchannels are amenable to the simple 1-tap frequency domain equalization, sub-channel-based detection, as well as bit and power loading for achieving channel capacity by waterfilling [3]. It is natural to integrate MIMO and OFDM in multi-antenna broadband communication systems [4][5].

Despite the much improved average capacity, wireless channel fading and noise effects can still result in substantial detection errors in MIMO-OFDM communications. To mitigate the potential detection errors due to distortive channel conditions and random noises, forward error correction (FEC) codes are routinely used in conjunction with MIMO-OFDM scheme. Over the past two decades, in particular, LDPC codes have received much attention for their excellent error-correcting performance [12], [13]. LDPC codes, when decoded via the sum-product algorithm (SPA), can approach Shannon limit performance with the practical decoding complexity [14].

When LDPC codes are applied within MIMO-OFDM [6], an ideal receiver should apply the joint maximum likelihood (ML) detection and decoding principle. However, when LDPC codes are sufficiently long, such an optimum joint receiver is highly complex and impractical to implement. The success of SPA decoding lies in its low complexity and good decoding performance for parity check matrices without short cycles. However, its iterative nature during message passing makes it a challenge to seamlessly integrate with the MIMO-OFDM detection step. As viable alternatives, the concept of turbo-equalization (or turbo detection) [7] has been proposed for the "quasi-joint" detection and decoding of LDPC coded MIMO-OFDM systems. The principle of turbo processing is to allow message passing between two individual processing blocks by replying on "belief propagation" (i.e., mutual trust during message passing). Turbo detection iteratively exchanges their soft information between MIMO-OFDM detector and the SPA decoder, often achieving near optimum performance without the high complexity of joint ML detection and decoding. Nevertheless, such a message exchange turbo receiver does

Manuscript received July 22, 2012; revised December 27, 2012 and March 31, 2013. The editor coordinating the review of this paper and approving it for publication was B. Clerckx.

This work was presented in part at the IEEE Global Communications Conference (GLOBECOM), Anaheim, California, Dec. 2012.

Y. Li was with the Department of Communication Engineering, Xiamen University, China, and the Department of Electronic and Computer Engineering, UC Davis, USA. He is now with the Key Lab of Mobile Communication in Chongqing, Chongqing University of Posts and Telecommunications (CQUPT), Chongqing, 400065 China (e-mail: yongli@cqupt.edu.cn).

L. Wang is with the Department of Communication Engineering, Xiamen University, Xiamen, 361005 China (e-mail: wanglin@xmu.edu.cn).

Z. Ding is with the Department of Electronic and Computer Engineering, UC Davis, USA (e-mail: zding@ucdavis.edu).

This material is based on works supported in part by China NSF under Grant 61271241 (for Y. Li and L. Wang), and based on works supported by US NSF under Grants CNS-0917251 and CNS1147930 (for Z. Ding).

Digital Object Identifier 10.1109/TCOMM.2013.050813.120530

not have a comprehensive or unified optimization formulation. The convergence of such iterative algorithm depends on the quality of the message passing and is thus less certain since exchanging unreliable information at moderate to low SNR may in fact harm both the detector and the decoder.

The major obstacle to deriving a uniform optimization criterion for joint detection and decoding of LDPC coded MIMO transmission lies in the fact that detection and decoding operate in two different (incompatible) fields. More specifically, detection typically aims to optimize in the complex (or real) field, whereas FEC decoding criterion is generally characterized in binary GF(2) field. Although it is less likely to translate detection criterion from complex field to binary field, some recent works on LDPC decoding have proposed new approaches based on linear programming (LP) decoding for linear (and particularly LDPC) codes [16]. By converting FEC binary constraints into linear inequalities in $\mathbb{R}$ or $\mathbb{C}$, LP decoding as well as reduced complexity algorithms [17][18][19] makes it possible to derive a unified optimization criterion for joint detection and decoding in LDPC coded MIMO-OFDM systems without relaying on message passing. In this work, we develop a new linear programming based receiver for joint detection and decoding of LDPC-coded data signals in MIMO-OFDM systems.

Linear programming decoder transforms binary code constraints into linear constraints in real field, thereby making it possible to be integrated with channel equalization and MIMO detection. The authors of [20] already developed a joint LP receiver for coded MIMO systems by using ℓ_1 norm as the detection metric that can be jointly considered with the LP decoding. Although the approach of [20] can also be generalized to coded MIMO-OFDM systems, the joint detection method of [20] requires a specific class of **affine mapping between the binary data bits** from the encoder and the modulated QAM symbols. In particular, such a linear mapping is found in BPSK and QPSK modulations. For the more general QAM signaling, the suggestion in [20] to decompose QAM into multiple affine-QPSK mappings, even for those atypical affine QAM mappings, would substantially increase computational complexity since it introduces a multiplicity of new variables in linear programming. More importantly, practically implemented QAM modulation (e.g., 16QAM) under Gray code does not permit such decomposition. In fact, for such QAM modulations, the mapping between input and output is generally nonaffine.

In this work, we generalize the joint detection-decoding algorithm for generic nonaffine QAM mapping to develop a new joint detection-decoding receiver for LDPC coded MIMO-OFDM systems. Without introducing many extra variables, we extend the treatment of nonaffine QAM mapping proposed in [22] for MIMO-OFDM systems. This approach makes it possible to deal with high-efficiency modulations that do not admit an affine input-output mapping and is a natural extension of the joint MIMO-LDPC receiver that we developed [23]. To begin, we derive a global objective function that is proportional to the probability density function of the transmission conditioned on the received observations. Next, according to the global function, we develop the corresponding factor graph. Finally, we propose an LP-based joint detection problem by extracting

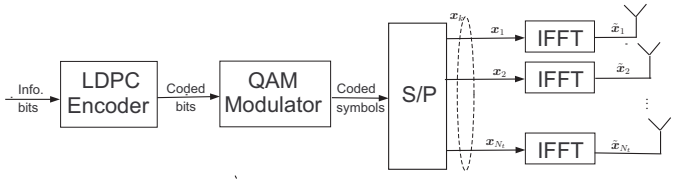

Fig. 1. Block diagram of an LDPC coded MIMO-OFDM transmission systems.

the LP variables and constraints directly from the factor graph. Compared with existing turbo equalization receivers (e.g. [7]) and known LP joint receivers (e.g. [20]), the new joint receiver exhibits strong error-rate performance.

We organize our manuscript as follows. In Section II, we briefly describe the system model of LDPC coded MIMO-OFDM transmission and summarize some known receivers for MIMO-OFDM detection and LDPC decoding. In Section III, we present our new LP based joint receiver for LDPC coded MIMO-OFDM systems and develop its factor graph. We discuss the complexity of the resulting algorithm. We test our new algorithms for joint receiver through numerical simulations in Section IV to demonstrate the receiver error performance before concluding our works in Section V.

II. System Description of LDPC Code MIMO-OFDM

A. Notations

In this manuscript, $(\cdot)^H$ and $(\cdot)^T$ denote the conjugate transpose and the transpose of a matrix, respectively. $\{\tilde{a}_t\}_{t=0,\ldots,N-1}$ denotes the N-point IFFT of symbol sequence $\{a_t\}_{t=0,\ldots,N-1}$.

B. Spatial Multiplexing MIMO Transmission

We consider an LDPC coded MIMO-OFDM transmission system of Figure 1, consisting of N_t transmit antennas, N_r receive antennas, and N subcarriers. The MIMO transmission takes the form of spatial multiplexing. As shown in Figure 1, a block of ℓ information bits is encoded by an LDPC encoder with code rate $\rho = \ell/n$. The output n coded bits are modulated by a Q-ary quadrature amplitude modulated (QAM) constellation into a block of n/Q QAM symbols. During each OFDM symbol time slot, $N_t \cdot N$ QAM symbol are transmitted from N subcarriers and N_t transmit antennas simultaneously. Let K be the number of OFDM symbol slots for this codeword of n bits, then $K = n/Q/(N_t N)$. Denote the index set of OFDM slots by $\mathcal{T}$, then $\mathcal{T} = \{0, 1, \ldots, K-1\}$.

The OFDM signal is obtained through IFFT precoding and cyclic prefix. The transmitted data

$$\tilde{\boldsymbol{x}}_i = \text{IFFT}_N\{\boldsymbol{x}_i\}, \tag{1}$$

where $\boldsymbol{x}_i = \{x_i(0), \ldots, x_i(N-1)\}$ denotes an OFDM symbol to be transmitted from the i-th transmit antenna, $1 \le i \le N_t$.

Define a modulation mapping as $\mathcal{M} : \{0,1\}^{Q\times 1} \longrightarrow \Gamma$ where $\Gamma \subset \mathbb{C}$ denotes the transmitted QAM constellation. For conveniently, we can define another mapping $\mathcal{X} : \{0,1\}^{QN_t\times 1} \longrightarrow \Gamma^{N_t\times 1}$ where every block of consecutive Q coded bits is mapped to a QAM symbol by the mapping

function $\mathcal{M}$. As shown in Figure 1, $\boldsymbol{x}_k$ denotes the frequency domain symbol vector for the k-th subcarrier obtained from $\boldsymbol{x}_k = \mathcal{X}(\boldsymbol{b})$ in which $\boldsymbol{b}$ is a vector of coded bits $\{b_i\}$ of length QN_t.

After applying FFT at the MIMO receiver, we obtain $\boldsymbol{r}_k$ as an $N_r \times 1$ symbol vector obtained from N_r receive antennas at the k-th subcarrier. Denote by $\boldsymbol{r}_k$ the received signal vector at the N_r receive antennas corresponding to the k-th subcarrier.

In OFDM, blocks of N data symbols are transformed by IFFT into blocks of N data symbols in time-domain. Each block of N data symbols further appends a cyclic prefix of length N_g before transmission. Recall that the cyclic prefix length N_g is chosen to overcome the inter-block interference (IBI) such that $N_g \geq L$ where L is the time-domain channel delay spread.

Let $\{H_{ji}(k)\}_{k=0,\ldots,N-1}$ be the N-point FFT of discrete time L-tap channel $\{h_{ji}(t),\ t = 0, \ldots, L-1\}$ between the i-th transmit antenna and the j-th receive antenna, written as

$$H_{ji}(k) = \sum_{t=0}^{L-1} h_{ji}(t) e^{-j\frac{2\pi}{N}kt}. \tag{2}$$

Channel coefficients $\{h_{ji}(t),\ t = 0, \ldots, L-1\}$ are modeled as an independent zero-mean complex Gaussian, satisfying mean power normalization constraint $E\left[\sum_{t=0}^{L-1} |h_{ji}(t)|^2\right] = 1$. The received signals from the j-th antenna after cyclic prefix removal and FFT transform become

$$r_j(k) = \sum_{i=1}^{N_t} H_{ji}(k)x_i(k) + n_j(k), \quad k = 0, 1, \ldots, N-1, \tag{3}$$

where $n_j(k)$ denotes the complex (frequency-domain) AWGN noise on the j-th receive antenna.

Because the time-domain channel noise is typically modeled as independent identically distributed (i.i.d.) Gaussian, $n_j(k)$ remains i.i.d. Gaussian after the unitary transform of FFT. By grouping the received symbols from all N_r receive antennas, we obtain N vectors $\boldsymbol{r}_k$ of size $N_r \times 1$, corresponding to N subcarriers, whose expression is as follows

$$\boldsymbol{r}_k = \mathbf{H}_k \boldsymbol{x}_k + \boldsymbol{n}_k, \quad k = 0, 1, \ldots, N-1, \tag{4}$$

in which $\boldsymbol{r}_k = [r_j(k)]_{1\leq j\leq N_r}$, $\boldsymbol{x}_k = [x_i(k)]_{1\leq i\leq N_t}$, $\boldsymbol{n}_k = [n_j(k)]_{1\leq j\leq N_r}$ and $\mathbf{H}_k = [H_{ji}(k)]_{\substack{1\leq j\leq N_r \\ 1\leq i\leq N_t}}$.

C. LDPC Error Correction Codes

An LDPC code $\mathcal{C}$ with parity check matrix P can be represented by a Tanner (or factor) graph $\mathcal{G} = (\mathcal{V}, \mathcal{E})$. Let $\mathcal{I} = \{1, 2, \ldots, m\}$ and $\mathcal{J} = \{1, 2, \ldots, n\}$, respectively, be the row and column indices of the parity check matrix P. The node set $\mathcal{V}$ can be partitioned into two disjoint node subsets indexed by $\mathcal{I}$ and $\mathcal{J}$, known as the check nodes and variable nodes, respectively. For each pair $(i, j) \in \mathcal{I}\times\mathcal{J}$, there exists an edge (i, j) in $\mathcal{G}$ if and only if the (i, j)-th element of the parity check matrix $P_{ij} = 1$. The index set of the neighborhood of a check node $i \in \mathcal{I}$ is defined as $\mathcal{N}_i := \{j \in \mathcal{J} : P_{ij} = 1\}$. Similarly, we denote $\mathcal{N}_j := \{i \in \mathcal{I} : P_{ij} = 1\}$ as the set of check nodes incident to a given variable node j. For each $i \in \mathcal{I}$, define the i-th local code (sometimes called local behavior) by

$$\mathcal{C}_i = \{(c_j)_{j\in\mathcal{N}_i} : \sum_{j\in\mathcal{N}_i} P_{i,j}c_j = 0\},$$

where $\mathcal{N}_i \subseteq \mathcal{I}$ is the support of the i-th row of P for each $i \in \mathcal{I}$, and addition and multiplication are over *GF*(2). Hence $\boldsymbol{c} \in \mathcal{C}$ if and only if $\boldsymbol{c}_i \triangleq (c_j)_{j\in\mathcal{N}_i}$ lies in $\mathcal{C}_i$ for each $i \in \mathcal{I}$, where $\boldsymbol{c}$ is a bit-vector with length of n. For more details, see [12], [22].

Because of the large code length, it is impractical to perform MAP decoding exactly for practical LDPC codes. Therefore, low complexity decoders are essential to the success of LDPC codes. Fortunately, the sum-product algorithm (SPA) [13], proves to be highly effective and efficient. In this paper, we use the very popular SPA in log-domain (LLR-SPA) [26].

The quantity $q^a_{i,j}, a \in \{0, 1\}$, denotes the probability that the variable node j has value a, based on the information obtained via all the checks except i. Similarly, $r^a_{i,j}$ denotes the probability of check i being satisfied when the variable node j is equal to a. Let $\boldsymbol{y} = [y_1, \ldots, y_n]$ be the received word corresponding to the transmitted codeword $\boldsymbol{c} = [c_1, \ldots, c_n]$. Furthermore, we define log-likelihood ratios (LLR) $\lambda_{j\to i}(c_j) \triangleq \log(q^0_{i,j}/q^1_{i,j})$ and $\Lambda_{i\to j}(c_j) \triangleq \log(r^0_{i,j}/r^1_{i,j})$. The LLR-SPA is then briefly summarized as follows.

Initialization: Assign an a posteriori LLR $L(c_j) = \log\{P(c_j = 0|y_j)/P(c_j = 1|y_j)\}$ to each variable node j. For each pair (i, j) with $P_{ij} = 1$,

$$\lambda_{j\to i}(c_j) = L(c_j), \Lambda_{i\to j}(c_j) = 0.$$

Step 1 (Horizontal step): For each i, and for each $j \in \mathcal{N}_i$, compute

$$\Lambda_{i\to j}(c_j) = 2\tanh^{-1}\{\prod_{j'\in N_i\setminus j} \tanh[\lambda_{j'\to i}(c_{j'})/2]\}; \tag{5}$$

Step 2 (Vertical step): For each j, and for each $i \in \mathcal{N}_j$, compute

$$\lambda_{j\to i}(c_j) = L(c_j) + \sum_{i'\in\mathcal{N}_j\setminus i} \Lambda_{i'\to j}(c_j); \tag{6}$$

For each j, compute

$$\lambda_j(c_j) = L(c_j) + \sum_{i\in\mathcal{N}_j} \Lambda_{i\to j}(c_j); \tag{7}$$

Step 3 (Decision): Quantize $\hat{\boldsymbol{c}} = [\hat{c}_1, \ldots, \hat{c}_n]$ such that

$$\hat{c}_j = \begin{cases} 0 & \text{if } \lambda_j(c_j) \geq 0 \\ 1 & \text{otherwise.} \end{cases}$$

If $\hat{\boldsymbol{c}}P^T = \mathbf{0}$, then the algorithm halts; Otherwise it returns to *Step 1*. If the algorithm does not halt beyond a preset maximum number of iterations, then declare a decoding failure.

In [27], [28], the concept of extrinsic information was originally introduced to identify the component of the generated reliability value which depends on redundant information obtained from the considered constituent code. In LLR-SPA, $\lambda_{j\to i}(c_j)$ represents the extrinsic information that variable

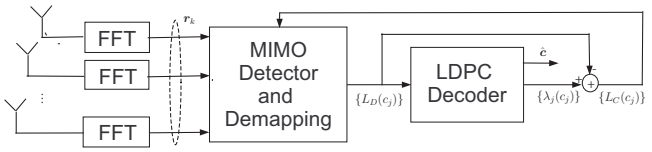

Fig. 2. Turbo receiver of LDPC coded MIMO-OFDM systems.

node j sends to check node i, and $\Lambda_{i\to j}(c_j)$ represents the extrinsic information that check node i sends to variable node j.

D. MIMO-OFDM Turbo Detection

The equalization and the detection of MIMO-OFDM signals are carried out in the real/complex field whereas the LDPC decoding is carried out in binary field GF(2). However, the soft-input-soft-output (SISO) nature of turbo decoding has paved one way of exchanging (extrinsic) information between the signal detection and SISO decoder based on the "belief propagation" principle. This iterative closed loop information exchange is known as turbo-equalization as proposed in [15], [29]. Figure 2 illustrates a standard MIMO turbo-equalization system.

This iterative receiver structure consists of a soft input soft output MIMO detector and an LLR-SPA decoder. Extrinsic information is exchanged between the two components in an iterative manner according to the belief propagation principle [15], [7]. Both the detection and the channel decoding are carried out in frequency-domain. In each turbo iteration, the MIMO detector computes the extrinsic LLR value of the coded bits and sends to the decoder; whereas the LLR-SPA decoder feeds the detector with an extrinsic information for the encoded bits that can be used as the a prior information to compute a soft estimate of transmitted symbols. In this paper, we use the MAP detector/equalizer. Assuming perfect channel state information (CSI) at the receiver, it is obvious from (2) and (4) that the detection of the received signals at a particular subcarrier can be carried out independently. For notational convenience, in the following, we temporarily drop the index of subcarriers (subscript k) from the signals in $\boldsymbol{r}$, $\mathbf{H}$, and $\boldsymbol{x}$ when there is no risk of confusion.

In the soft MAP detector, received data $\boldsymbol{r}$ for each subcarrier is demapped by a log-likelihood ratio (LLR) calculation for each bit of the N_tQ coded bits in the transmit symbol vector $\boldsymbol{x}$. The extrinsic LLR value of the estimated bit c_j ($j \in \{1,\ldots,N_tQ\}$) is computed as

$$\begin{aligned} L_D(c_j) &= \log\frac{P(c_j=+1|\boldsymbol{r},\mathbf{H})}{P(c_j=-1|\boldsymbol{r},\mathbf{H})} - \log\frac{P(c_j=+1)}{P(c_j=-1)} \\ &= \log\frac{\sum_{\boldsymbol{x}\in\chi_j^{+1}} P(\mathbf{r}|\boldsymbol{x},\mathbf{H})P(\boldsymbol{x})}{\sum_{\boldsymbol{x}\in\chi_j^{-1}} P(\boldsymbol{r}|\boldsymbol{x},\mathbf{H})P(\boldsymbol{x})} - L_C(c_j), \quad (8) \end{aligned}$$

where $L_C(c_j)$ is the extrinsic information of the bit c_j from the LDPC decoder in the previous turbo iteration (at the first iteration $L_C(c_j) \equiv 0, \forall j$); χ_j^{+1} denotes the set of 2^{N_tQ-1} vector $\boldsymbol{x}$ having $c_j = +1$, while χ_j^{-1} denotes the complementary set. Assuming the bits within $\boldsymbol{x}$ are mutually independent, the a priori probability $P(\boldsymbol{x})$ can be computed as

$$P(\boldsymbol{x}) = \prod_{j=1}^{N_tQ} P(c_j) = \prod_{j=1}^{N_tQ} [1+\exp(-x_j L_C(c_j))]^{-1}, \quad (9)$$

where x_j corresponds to the j-th binary bit in symbol vector $\boldsymbol{x}$. The probability density function $P(\boldsymbol{r}|\boldsymbol{x},\mathbf{H})$ is Gaussian. The extrinsic information $L_C(c_j)$ can be computed as

$$L_C(c_j) = \lambda_j(c_j) - L_D(c_j), \quad (10)$$

where $\lambda_j(c_j)$ is determined by (7), and $L(c_j)$ in (7) is replaced by $L_D(c_j)$.

After each turbo iteration, the decoder verifies whether $\hat{\boldsymbol{c}}$ is a valid codeword. If true, the MIMO-OFDM turbo equalization halts; otherwise, turbo equalization continues until a maximum number of turbo iterations. The soft MAP detector in (8) has a complexity of $O(2^{N_tQ})$ and is suitable for modest constellation size and limited number of transmit antennas in practice.

Despite the general success of turbo detection, it has some weaknesses. Firstly, it is not yet clear how many iterations are needed for turbo detection to converge. Secondly, turbo detection often suffers from performance degradation because of local instead of global optimal solution. Poor local convergence is a direct consequence of "belief propagation" when the passed messages are inaccurate and often exhibits error floor in high SNR region. Thirdly, the performance of turbo detection is difficult to anticipate and analyze. To mitigate these shortcomings, we now investigate a new joint MIMO-OFDM detection and decoding algorithm that relies on a single unified objective function for optimization.

III. LP Based Joint MIMO-OFDM Receiver

A. QAM Signals under Affine Mapping

We aim to develop a unified objective function for LDPC-coded QAM signal transmissions in MIMO-OFDM systems. Recall the linear input/output relationship of MIMO-OFDM receivers. We use $\hat{\mathbf{H}}_t(k)$, $\hat{\boldsymbol{x}}_t(k)$ and $\hat{\boldsymbol{r}}_t(k)$, respectively, to denote the channel, the transmitted symbol vector and the received data, respectively, at the t-th transmit slot and k-th subcarrier. Staying in field $\mathbb{R}$, we can write the input/output relationship as

$$\hat{\boldsymbol{r}}_{t,k} = \hat{\mathbf{H}}_{t,k}\hat{\boldsymbol{x}}_{t,k} + \hat{\boldsymbol{n}}_{t,k} \quad (11)$$

where

$$\hat{\boldsymbol{r}}_{t,k} = \begin{bmatrix} \mathrm{Re}\{\boldsymbol{r}_{t,k}\} \\ \mathrm{Im}\{\boldsymbol{r}_{t,k}\} \end{bmatrix}, \hat{\boldsymbol{x}}_{t,k} = \begin{bmatrix} \mathrm{Re}\{\boldsymbol{x}_{t,k}\} \\ \mathrm{Im}\{\boldsymbol{x}_{t,k}\} \end{bmatrix} \quad (12)$$

and

$$\hat{\boldsymbol{n}}_{t,k} = \begin{bmatrix} \mathrm{Re}\{\boldsymbol{n}_{t,k}\} \\ \mathrm{Im}\{\boldsymbol{n}_{t,k}\} \end{bmatrix}, \hat{\mathbf{H}}_{t,k} = \begin{bmatrix} \mathrm{Re}\{\mathbf{H}_{t,k}\} & -\mathrm{Im}\{\mathbf{H}_{t,k}\} \\ \mathrm{Im}\{\mathbf{H}_{t,k}\} & \mathrm{Re}\{\mathbf{H}_{t,k}\} \end{bmatrix}. \quad (13)$$

From the relationship of (11), the LP joint detector for coded MIMO systems introduced in [20] can be easily generalized to coded MIMO-OFDM systems by minimizing

$$\sum_t \sum_k |\hat{\mathbf{H}}_{t,k}\cdot\hat{\boldsymbol{x}}_{t,k} - \hat{\boldsymbol{r}}_{t,k}|.$$

In other words, we now have a linear programming detection formulation:

$$\min \sum_{t\in\mathcal{T}}\sum_{k=0}^{N-1}\sum_{i=1}^{2N_r}\tau_{t,k,i} \tag{14}$$

$$s.t.\ |\hat{\mathbf{H}}_{t,k}\cdot\hat{\boldsymbol{x}}_{t,k}-\hat{\boldsymbol{r}}_{t,k}|\le\tau_{t,k}=\begin{bmatrix}\tau_{t,k,1}\\ \vdots\\ \tau_{t,k,2N_r}\end{bmatrix},$$
$$\forall t\in\mathcal{T}, 0\le k\le N-1, \tag{15}$$

where $\{\tau_{t,k,i}\}$ and $\{\hat{\boldsymbol{x}}_{t,k}\}$ are our LP variables.

$\{\hat{\boldsymbol{x}}_{t,k}\}$ in (15) is related to the given code $\mathcal{C}$. The corresponding codeword polytope can be defined to be the convex hull of all possible codewords

$$\text{poly}(\mathcal{C})=\left\{\sum_{\boldsymbol{c}\in\mathcal{C}}\lambda_{\boldsymbol{c}}\boldsymbol{c}:\lambda_{\boldsymbol{c}}\ge 0,\sum_{\boldsymbol{c}\in\mathcal{C}}\lambda_{\boldsymbol{c}}=1\right\}.$$

Note that poly$(\mathcal{C})$ includes exactly those vertices corresponding to codewords, and every point in poly$(\mathcal{C})$ corresponds to a vector $\boldsymbol{f}=(f_1,\ldots,f_n)$ where component f_i is defined in terms of the summation $f_j=\sum_{\boldsymbol{c}}\lambda_{\boldsymbol{c}}c_j$. This polytope can be represented by a finite number of linear constraints; however, the number of constraints is exponential in the code length n. To reduce the complexity, poly$\{\mathcal{C}\}$ can be relaxed onto the so-called fundamental polytope obtained by intersecting the convex hull of local codewords corresponding to each row of the parity check matrix [16]. It can be characterized by the following inequalities:

$$0\le f_j\le 1,\qquad \forall j\in\mathcal{J}; \tag{16}$$

and

$$\sum_{j\in\mathcal{F}}f_j-\sum_{j\in\mathcal{N}_i\setminus\mathcal{F}}f_j\le|\mathcal{F}|-1,\qquad\forall i\in\mathcal{I},\forall\mathcal{F}\subset\mathcal{N}_i,|\mathcal{F}|\text{odd}. \tag{17}$$

Together with the LP detection formulation and assume QPSK modulation, we can summarize the first detector as a generalization of the method in [20] as

LP1: Joint MIMO-OFDM Equalization and Decoding by ℓ_1 norm

$$\min \sum_{t\in\mathcal{T}}\sum_{k=0}^{N-1}\sum_{i=1}^{2N_r}\tau_{t,k,i} \tag{18}$$

Constraints: (16), (17) and

$$\tau_{t,k,i}\ge 0,\forall t\in\mathcal{T},\forall k\in[0,N-1],\forall i\in[1,2N_r], \tag{19}$$

$$\hat{\mathbf{H}}_{t,k}\hat{\boldsymbol{x}}_{t,k}-\boldsymbol{\tau}_{t,k}\le\hat{\boldsymbol{r}}_{t,k}-\hat{\mathbf{H}}_{t,k}\hat{\boldsymbol{x}}_{t,k}-\boldsymbol{\tau}_{t,k}\le-\hat{\boldsymbol{r}}_{t,k},\quad\forall t\in\mathcal{T},\forall k\in[0,N-1]\} \tag{20}$$

$$\text{Re}\{\hat{\boldsymbol{x}}_{t,k}\}=\sqrt{1/2}\big[1-2f_{t(N\cdot N_t\cdot 2)+k\cdot N_t\cdot 2+1},\ldots,1-2f_{t(N\cdot N_t\cdot 2)+k\cdot N_t\cdot 2+2N_t-1}\big]^T$$
$$\text{Im}\{\hat{\boldsymbol{x}}_{t,k}\}=\sqrt{1/2}\big[1-2f_{t(N\cdot N_t\cdot 2)+k\cdot N_t\cdot 2+2},\ldots,1-2f_{t(N\cdot N_t\cdot 2)+k\cdot N_t\cdot 2+2N_t}\big]^T,$$
$$\forall t\in\mathcal{T},\forall k\in[0,N-1] \tag{21}$$

In **LP1**, note that $\{\tau_{t,k,i}\}$ and $\{f_j\}$ are the optimization variables.

Assume for simplicity that the parity-check matrix of the LDPC code has a constant number w_r of nonzero elements in each row. Then in terms of computational complexity, **LP1** consists of $n+2KNN_r$ variables and $4KNN_r+m2^{w_r-1}$ constraints.

The algorithm **LP1** is a linear programming method only when there is an affine mapping between f_j and $\hat{\boldsymbol{x}}_{t,k}$. It is obvious that **LP1** is only suitable for affine mapping (say BPSK, QPSK). As for higher order modulation with non-constant modulus such as 16QAM, the authors in [20] suggested to decompose a 16QAM modulated symbol into two QPSK symbols [24]. Not only this decomposition doubles the number of variables in the LP detector, but such a decomposition is also not generally feasible when practical nonaffine mappings such as Gray code is used. Moreover, **LP1** does not admit the so-called *maximum likelihood certificate* property, which is the most appealing property of LP decoding.

B. Factor Graph and the Derivation of LP Receiver for Nonaffine QAM Mapping

For broad applications in practical MIMO-OFDM systems, we wish to formulate a joint receiver regardless of affine or nonaffine QAM modulation mapping. We would also like such a joint detector to retain the *maximum likelihood certificate* property under some special conditions. We have recently presented some preliminary work in [23]. In this manuscript, we generalize our preliminary paper [23] on MIMO detection under flat fading channel to the more general MIMO-OFDM systems that can accommodate frequency selective fading channels.

Recall that the authors of [22] designed a detector of jointly considering the equalizer and decoder over frequency selective channels. In the method of [22], the global function was factorized as the products of some real-valued functions and indicator functions. The real-valued functions and the indicator functions correspond to the cost function and the constraints of linear programming, respectively. By expanding this approach into joint detection and decoding, nonaffine mapping can be tackled through the introduction of some auxiliary variables.

The method in [22] can be generalized for joint detection and decoding in the LDPC-coded MIMO-OFDM systems. In what follows, we will detail our joint detection. First we derive the factor graph for the LDPC coded MIMO-OFDM systems. QN_t coded bits are modulated (every Q bits corresponding to a symbol) and transmitted on each subcarrier from N_t antennas at each OFDM slot. Denote the coded bits vector with length of QN_t corresponding to the symbol vector consisting of N_t symbols from N_t antennas at t-th slot and k-th subcarrier by $\boldsymbol{s}_{t,k}, t\in\mathcal{T}, k\in[0,N-1]$. There are $|\Gamma|^{N_t}$ different symbol vectors since each QAM symbol in $\boldsymbol{s}_{t,k}$ has $|\Gamma|=2^Q$ possible values. Let $\mathcal{S}$ be a set consisting of all the vector elements corresponding to the bit vector $\boldsymbol{s}_{t,k}$, and let $\mathcal{S}^-=\mathcal{S}\setminus\mathbf{0}_{1\times QN_t}$ where $\mathbf{0}_{1\times QN_t}$ represents an all-zero vector of length QN_t.

Assuming that each codeword is transmitted with equal probability. By using Bayes rule, a posteriori probability

(APP) of the transmitted codeword $\boldsymbol{s}$ conditioned on the entire received vector can be written as

$$P(\boldsymbol{s}|\boldsymbol{r}) = \frac{p(\boldsymbol{r}|\boldsymbol{s}) \cdot P(\boldsymbol{s})}{p(\boldsymbol{r})}. \tag{22}$$

Consequently, we define a global function as

$$\begin{aligned} u(\boldsymbol{s}) &= p(\boldsymbol{r}|\boldsymbol{s}) \\ &= p(\boldsymbol{r}_{0,0}, \ldots, \boldsymbol{r}_{0,N-1}, \ldots, \boldsymbol{r}_{K-1,0}, \ldots, \boldsymbol{r}_{K-1,N-1}| \\ &\quad \boldsymbol{s}_{0,0}, \ldots, \boldsymbol{s}_{0,N-1}, \ldots, \boldsymbol{s}_{K-1,0}, \ldots, \boldsymbol{s}_{K-1,N-1}) \\ &= \prod_{t\in\mathcal{T}} \left(\prod_{k=0}^{N-1} Q_{t,k}(\boldsymbol{s}_{t,k}) \right) \cdot \prod_{i\in\mathcal{I}} \Psi_i(\boldsymbol{s}_i). \end{aligned} \tag{23}$$

Here $Q_{t,k}(\boldsymbol{s}_{t,k}) = p(\boldsymbol{r}_{t,k}|\boldsymbol{s}_{t,k})$ for each $t \in \mathcal{T}$ and each $k \in [0, N-1]$ is a multivariate Gaussian probability density function, and all factor nodes $\Psi_i(\boldsymbol{s}_i)$ for each $i \in \mathcal{I}$ are indicator functions for some local behavior $\mathcal{C}_i$, i.e.,

$$\Psi_i(\boldsymbol{s}_i) = \begin{cases} 1, & \text{if } \boldsymbol{s}_i \in \mathcal{C}_i; \\ 0, & \text{otherwise;} \end{cases} \qquad \forall i \in \mathcal{I},$$

where $\boldsymbol{s}_i$ has the similar definition as $\boldsymbol{c}_i$ in Section II. The second term of the last equality in (23) guarantees that $\boldsymbol{s}$ is a valid codeword. Then $\hat{\boldsymbol{s}} = \text{argmax}_{\boldsymbol{s}\in\mathcal{C}} u(\boldsymbol{s})$ is the ML solution.

From (23) we know

$$\begin{aligned} \max\ u(\boldsymbol{s}) \Leftrightarrow & \max \prod_{t\in\mathcal{T}} \left(\prod_{k=0}^{N-1} Q_{t,k}(\boldsymbol{s}_{t,k}) \right) \cdot \prod_{i\in\mathcal{I}} \Psi_i(\boldsymbol{s}_i) - \\ & \prod_{t\in\mathcal{T}} \left(\prod_{k=0}^{N-1} Q_{t,k}(\boldsymbol{0}_{1\times QN_t}) \right) \\ = & \max \sum_{t\in\mathcal{T}} \sum_{k=0}^{N-1} \left(\log \frac{Q_{t,k}(\boldsymbol{s}_{t,k})}{Q_{t,k}(\boldsymbol{0}_{1\times QN_t})} \right) \cdot \prod_{i\in\mathcal{I}} \Psi_i(\boldsymbol{s}_i) \\ = & \max \sum_{t\in\mathcal{T}} \sum_{k=0}^{N-1} \left(\sum_{\boldsymbol{\alpha}\in\mathcal{S}} q_{t,k,\boldsymbol{\alpha}} \log \frac{Q_{t,k}(\boldsymbol{\alpha})}{Q_{t,k}(\boldsymbol{0}_{1\times QN_t})} \right) \cdot \\ & \prod_{i\in\mathcal{I}} \Psi_i(\boldsymbol{s}_i) \end{aligned} \tag{24}$$

where the first expression is valid because the second term of its right hand side is a constant, and $q_{t,k,\boldsymbol{\alpha}}$ is defined as

$$q_{t,k,\boldsymbol{\alpha}} = P\{\boldsymbol{s}_{t,k} = \boldsymbol{\alpha}\}.$$

It should be pointed out that the introduction of auxiliary variables $\{q_{t,k,\boldsymbol{\alpha}}\}$ is to facilitate the description of aftermentioned LP-based detectors. Because the coded bits vector transmitted in slot-t and subcarrier-k is fixed (although unknown), the set $\{q_{t,k,\boldsymbol{\alpha}} : \boldsymbol{\alpha} \in \mathcal{S}\}$ only has a single nonzero element, which equals '1'. In the following, we derive a factor graph corresponding to (24). Without loss of generality, let us illustrate with the special example of a binary (8, 4) extended Hamming code, QPSK mapping and focus on the case with only two transmit antennas and two subcarriers. The corresponding factor graph of the global function (24) is illustrated in Figure 3. The circle nodes, namely $c_1, c_2, \ldots, c_8$, $q_{1,0,\boldsymbol{s}_{1,0}}$ and $q_{1,1,\boldsymbol{s}_{1,1}}$ denote variables, the factor nodes with degree-1 correspond to the cost function, and left factor nodes Ψ_1, Ψ_2, Ψ_3 and Ψ_4 correspond to the constraints. It should be noted that $q_{1,0,\boldsymbol{s}_{1,0}}$ and $q_{1,1,\boldsymbol{s}_{1,1}}$ both correspond to $|\mathcal{S}| = 16$ optimized variables, respectively, because $\boldsymbol{s}_{1,0}$ and $\boldsymbol{s}_{1,1}$ both have 16 possible values. That is, there are 24 optimization variables in total. The factor node Ψ_1 represents the first row of parity-check matrix of the extended Hamming code. As shown in Figure 3, the variable nodes c_2, c_3, c_4 and c_5 form a check equation, i.e., $c_2 \oplus c_3 \oplus c_4 \oplus c_5 = 0$. Ψ_2, Ψ_3 and Ψ_4 have the similar definitions. Every two consecutive coded bits are grouped and mapped into a QPSK symbol, and every two QPSK symbols from two transmit antennas are grouped into a vector. It is equivalent that every four (QN_t) consecutive coded bits are grouped into a vector $\boldsymbol{\alpha}$. This vector is mapped by the mapping function $\mathcal{X}$ and sent by transmit antennas. Ψ_1, Ψ_2, Ψ_3 and Ψ_4 guarantee that $\boldsymbol{c} = (c_1, c_2, \ldots, c_8)$ is a valid codeword.

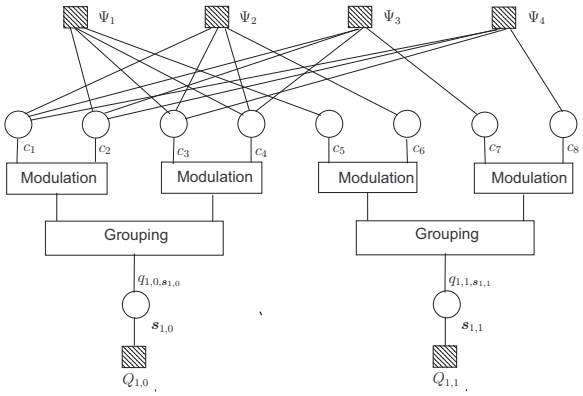

Fig. 3. Factor graph for coded MIMO-OFDM systems.

From the factor graph, we can derive the following LP problem directly for LDPC-encoded MIMO-OFDM systems by relaxing the aforementioned optimization variables with the box constraint $0 \le x \le 1$ where x is an optimization variable.

LP2: New Joint Detector for LDPC coded MIMO-OFDM systems

$$\max \sum_{t\in\mathcal{T}} \sum_{k=0}^{N-1} \sum_{\boldsymbol{\alpha}\in\mathcal{S}^-} \lambda_{t,k}^{(\boldsymbol{\alpha})} q_{t,k,\boldsymbol{\alpha}} \tag{25}$$

Constraints: (16), (17) and

$$\sum_{\boldsymbol{\alpha}\in\mathcal{S}} q_{t,k,\boldsymbol{\alpha}} = 1, \forall t \in \mathcal{T}, \forall k \in [0, N-1]; \tag{26}$$

$$q_{t,k,\boldsymbol{\alpha}} \ge 0, \forall t \in \mathcal{T}, \forall k \in [0, N-1], \forall \boldsymbol{\alpha} \in \mathcal{S}; \tag{27}$$

$$\sum_{\boldsymbol{\alpha}\in\mathcal{S}:\boldsymbol{\alpha}_l=1} q_{t,k,\boldsymbol{\alpha}} = f_{(t\cdot N+k)\cdot QN_t+l}, \forall t \in \mathcal{T}, \forall k \in [0, N-1], \forall l \in \{1, 2, \ldots, QN_t\}. \tag{28}$$

Receiver output

$$\boldsymbol{c}_{out} = \begin{cases} \boldsymbol{f}, & \text{if } \boldsymbol{f} \text{ is integer;} \\ \text{Failure,} & \text{otherwise.} \end{cases} \tag{29}$$

In **LP2**, $\{q_{t,k,\boldsymbol{\alpha}}\}$ and $\{f_j\}$ are optimization variables, whereas

weighting $\lambda_{t,k}^{(\boldsymbol{\alpha})}$ can be computed by

$$\begin{aligned}\lambda_{t,k}^{(\boldsymbol{\alpha})} &= \log\frac{Q_{t,k}(\boldsymbol{\alpha})}{Q_{t,k}(\mathbf{0}_{1\times QN_t})} \\ &\propto \frac{\sum_{m=1}^{N_r}|r_{t,k,m}-\mathbf{H}_{t,k}[m,:]X(\mathbf{0})|^2}{\sigma^2} - \\ &\quad \frac{\sum_{m=1}^{N_r}|r_{t,k,m}-\mathbf{H}_{t,k}[m,:]X(\boldsymbol{\alpha})|^2}{\sigma^2}. \end{aligned} \quad (30)$$

Here $\mathbf{H}_{t,k}[m,:]$ represents the m-th row of $\mathbf{H}_{t,k}$.

When all the auxiliary variables $\{q_{t,k,\boldsymbol{\alpha}}\}$ acquire binary values $\{0, 1\}$ in the LP solution, from (28) we know that $\boldsymbol{f}$ is a binary integer vector and thus is a valid codeword. As a result, (25) is equivalent to (24). It means that $\boldsymbol{f}$ is an ML codeword. This implies that **LP2** has the *maximum likelihood certificate* property.

In terms of complexity, we can quantify the number of LP variables and constraints directly. Assuming for simplicity that there are a fixed number w_r of nonzero elements in each row of the parity-check matrix of the LDPC code, **LP2** consists of $n + KN2^{QN_t}$ variables and $KN + n + m2^{w_r-1}$ constraints.

C. Complexity Reduction

It is easily seen from (17) that there are 2^{d_c-1} constraints corresponding to each check node of degree d_c. Therefore, the total number of constraints and consequently, the complexity of the joint detection and decoding problem, grow exponentially with the maximum check node degree $d_c^{\max}$. To reduce the computational complexity in our receiver, we can drop constraints defined by (17) when implementing **LP1** and **LP2**, and apply the ALP method [17] in which only useful constraints are added to the LP problem in an adaptive and iterative method. To keep things simple, we use the same notations, i.e, **LP1** and **LP2**. Using the ALP method, **LP2** includes the following steps:

(S1) Compute $\lambda_{t,k}^{(\boldsymbol{\alpha})}$ according to (30).
(S2) Initialize LP detection problem with constraints from (16), (26) and (28); set $m = 1$.
(S3) Solve the current LP problem to obtain the solution $\mathbf{c}_m$.
(S4) If no cut (so-called useful constraint) is found, stop; Otherwise, add the violated parity inequalities to the problem, set $m = m + 1$, and return to (S3).

Similarly, **LP1** can also be simplified using ALP for lower complexity.

The adaptive procedure of the above joint detection and decoding problem is similar to the adaptive method of LP decoding in [17] except that it starts from (26) and (28) instead of $2n$ box constraints. Thus, **LP2** converges after at most n iterations and the final application of LP solver in the **LP2** uses at most $KN + n(m + 1)$ constraints, which can be directly obtained from *Theorem* 2 and *Corollary* 1 in [17].

It should be pointed out that the use of ALP does not lead to frame error rate (FER) improvement. However, it has a very positive effect on speed of convergence because of the fewer constraints are enforced without (17). We also note that only the parity inequalities corresponding to each row of parity check matrix P are checked in **LP2**. Actually, during the process of solving **LP2**, sometimes a pseudo-codeword is obtained but no cut can be found. However, some parity inequalities corresponding to redundant parity checks are in fact violated. This means that certain fractional (pseudo-codeword) solution can be prevented by adding the violated redundant parity checks (RPCs) into **LP2** and solving the LP problem which now integrates the new linear code constraints from the RPCs. This way, we can further improve the error-rate performance of **LP2** by introducing redundant parity checks, as suggested in [18], [19].

When using the ACG-ALP method proposed in [19], we arrive at a more robust detector named henceforth which we label as **LP3** that can achieve better performance at higher complexity. We shall demonstrate the performance of both **LP2** and **LP3** receivers in our simulations.

IV. Simulation Results

In this section we provide some simulation results of the proposed joint receivers **LP2** and **LP3**. We implement the joint receivers by C++, and use the simplex method from the open-source GNU Linear Programming Kit (GLPK) as our LP solver [30]. In the coded MIMO-OFDM systems, We consider three random LDPC codes, constructed to avoid length-4 short cycles [25]. We consider 3 different LDPC codes in our tests. Let r, n, and γ, respectively, denote the rate, the length, and the column weight of LDPC codes. The 3 LDPC codes are

$$\begin{aligned}&\text{Code } C_1: \quad r = 1/2, \quad n = 256, \quad \gamma = 3;\\ &\text{Code } C_2: \quad r = 1/2, \quad n = 512, \quad \gamma = 3;\\ &\text{Code } C_3: \quad r = 3/4, \quad n = 512, \quad \gamma = 3.\end{aligned}$$

Both QPSK and 16QAM modulations are tested with three different antenna configurations: two transmit and two receive antennas (2×2), four transmit and three receive antennas (3×4) and four transmit and four receive antennas (4×4). In our simulations, for each OFDM slot of every block, we generate the time domain multi-path Rayleigh channels with randomly generated time-domain FIR channel coefficients. Unless specified explicitly, we consider 3-tap FIR multi-path channels in our tests. We assume the Rayleigh fading channels remain static during each OFDM slot but vary independently from one OFDM slot to another. We also set the number of OFDM subcarriers to 32 in our experiments.

As a comparison, we also test two other joint receivers based on **LP1** and turbo equalization (TE) consisting of MAP equalization and SPA decoding. In our subsequent simulations of turbo equalization, to avoid saturating operations, we implement LLR-SPA by using the method proposed in [31].

Since **LP1** requires affine mapping, its performance is only shown for comparison when QPSK modulation is used. When nonaffine QAM mapping is used, turbo equalization serves as a benchmark against our **LP2** and **LP3** receivers. For random LDPC codes, the SPA decoder with 10 iterations often achieves excellent performance. Therefore, we fix the local block iterations within the turbo equalizer to 10 unless otherwise specified. The number of turbo iterations is also set to 10 empirically to allow good convergence.

A. Example 1

We demonstrate the comparative (BER/FER) performances of the four different joint receivers with code C_1 under two

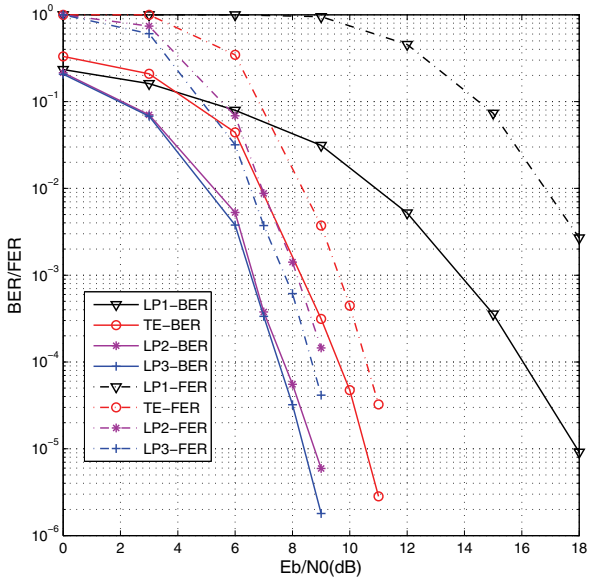

Fig. 4. BER (solid lines) and FER (dot-dashed lines) performance comparison of LDPC coded MIMO-OFDM systems with code C_1, QPSK modulation, 2 transmit and 2 receive antennas.

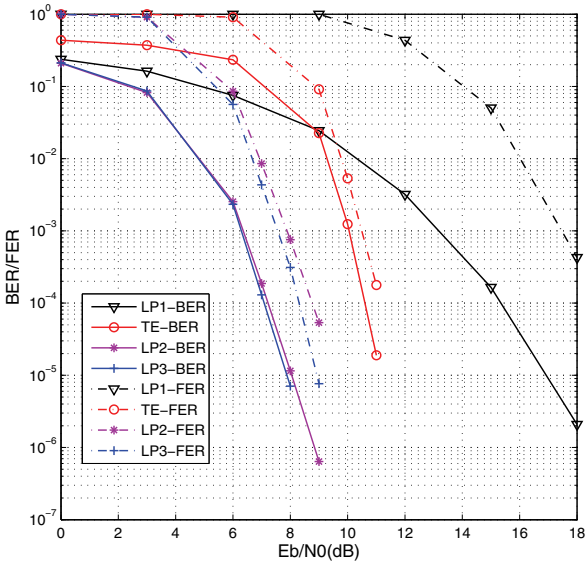

Fig. 5. BER (solid lines) and FER (dot-dashed lines) performance comparison of LDPC coded MIMO-OFDM systems with code C_1, QPSK modulation, 4 transmit and 4 receive antennas.

antenna configurations in Figures 4-5 when QPSK modulation is used. From the results, we can see from Fig. 4 that, at BER of 1×10^{-5}, our proposed joint detector **LP2** achieves a performance gain of approximately 9.3 dB and 1.8 dB over the algorithm in [20] and the turbo equalization, respectively. Furthermore, **LP3** exhibits nearly 0.4 dB gain when compared with **LP2**. Moreover, in terms of FER, **LP2** exhibits over 10.0 dB gain over **LP1**, while **LP3** has about 2.0 dB gain than TE. The improvement of **LP2** over **LP1** originates from the fact that **LP2** aims to directly optimize the global function which is consistent with maximum likelihood, whereas **LP1** is derived from an approximation of the global function (i.e, ℓ_1 norm). On the other hand, the improvement of **LP3** over **LP2** is a direct consequence from the inclusion of additional redundant parity checks as linear constraints to tighten the solution set.

Fig. 5 compares the performance of four detectors in 4×4 MIMO-OFDM systems. We again observe the advantage of our proposed joint detection algorithm as **LP2** outperforms **LP1** and TE by about 9.0 dB and 3.0 dB, respectively, at BER of 1×10^{-5}. In this case, **LP3** is only slightly better than **LP2**. In terms of FER, **LP2** is more than 10.0 dB and 2.0 dB better than **LP1** and TE, respectively, at FER $\leq 10^{-3}$. At the same setting, **LP3** provides up to 3.0 dB gain over TE. We see that our proposed detectors perform well when more transmit and receive antennas are used.

We can compare the complexities of LP1 and LP2 loosely by listing the number of variables and constraints. Under 2×2 MIMO, regardless of the parity check constraints, **LP1** has $n + 2KNN_r = 512$ variables and $4KNN_r = 512$ constraints. On the other hand, **LP2** consists of $n + KN2^{QN_t} = 1280$ variables and 320 constraints. Although a direct complexity comparison is not easy for such problems, our computer runtime tests show that the complexities of both LP detectors are comparable. In our tests, we found that the number of constraints has stronger impact on the complexity of an LP problem compared with the number of variables.

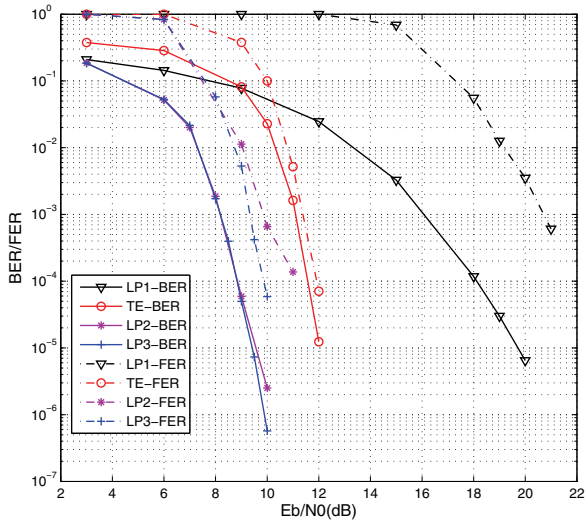

Fig. 6. BER (solid lines) and FER (dot-dashed lines) performance comparison of LDPC coded MIMO-OFDM systems with code C_2, QPSK modulation, 4 transmit and 3 antennas.

B. Example 2

We now compare the four receiver algorithms with another two codes C_2 and C_3 in Fig. 6-7 when 4 transmit antennas and 3 receive antennas are used. In these two examples, the number of receive antennas is smaller than that of transmit antennas. Thus, the MIMO channels have weaker diversity. From Fig. 6, we observe that **LP2** performs nearly 11.0 dB and 1.6 dB better than **LP1** and TE, respectively, at FER of 10^{-3}. However, **LP2** appears to show an error floor when FER $\leq 6 \times 10^{-4}$ and only outperforms TE by 1.0 dB at FER of 2×10^{-4}. On the other hand, **LP3** has about 2.0 dB gain over TE in the tested SNR range. We also observe similar

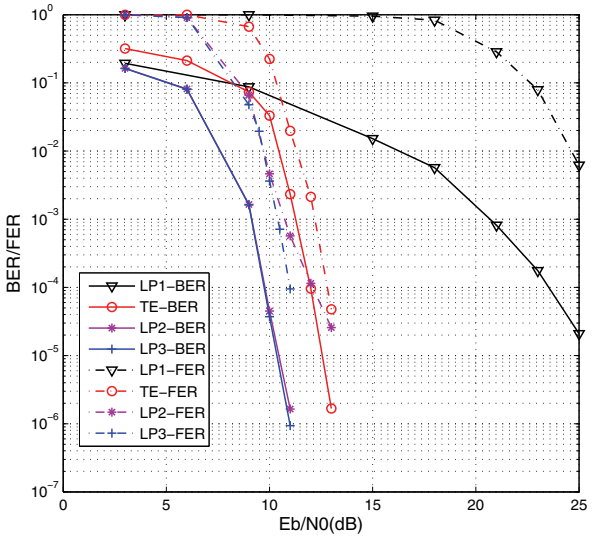

Fig. 7. BER (solid lines) and FER (dot-dashed lines) performance comparison of LDPC coded MIMO-OFDM systems with code C_3, QPSK modulation, 4 transmit and 3 antennas.

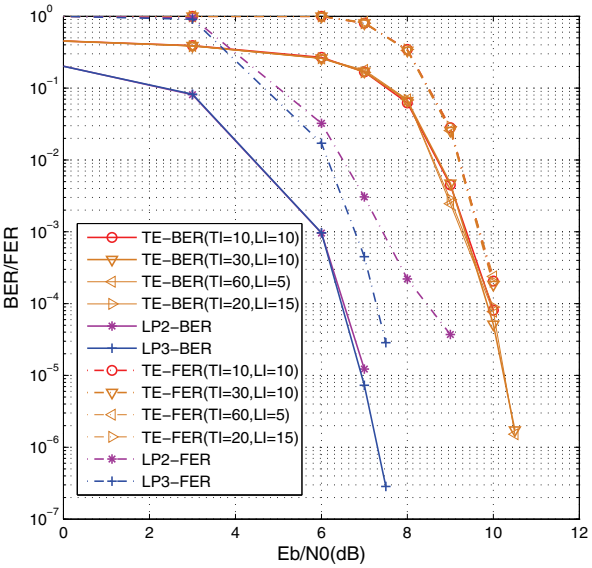

Fig. 8. BER (solid lines) and FER (dot-dashed lines) performance comparison between proposed joint detectors and TE in 3-tap frequency selective channels with code C_2, QPSK modulation, 4 transmit and 4 antennas.

performance relationship of the 4 detectors when using another high-rate code C_3 in Fig. 7.

C. Example 3

To illustrate the advantages of our joint detectors over TE in greater detail, in Figures. 8-9 we present the BER/FER performance of proposed joint detectors and TE using code C_2 in a 4×4 MIMO-OFDM system. We see from Fig. 8 that TE has the similar performance when different combinations of the number of local iterations (LI) and the number of turbo iterations (TI) are used, respectively. It means that TE cannot be further improved obviously by increasing the number of turbo iterations or local iterations beyond what was sufficient. **LP2** and **LP3** outperform TE more than 3.0 dB at BER of 10^{-5}. Moreover, **LP2** appears an error floor at FER $\leq 2 \times$

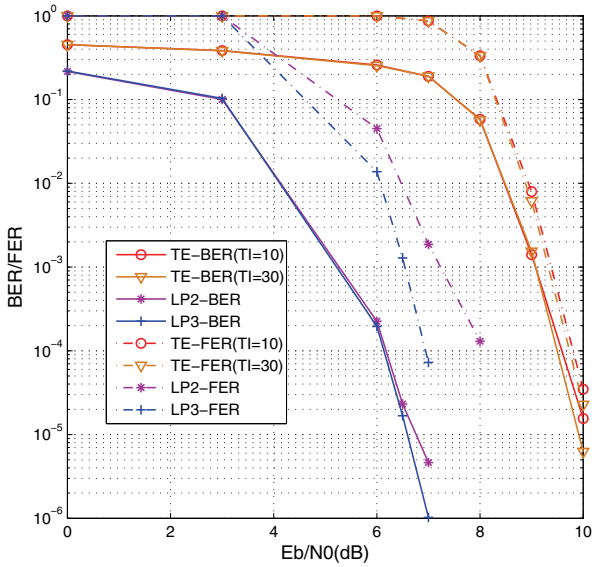

Fig. 9. BER (solid lines) and FER (dot-dashed lines) performance comparison between proposed joint detectors and TE in 5-tap frequency selective channels with code C_2, QPSK modulation, 4 transmit and 4 antennas.

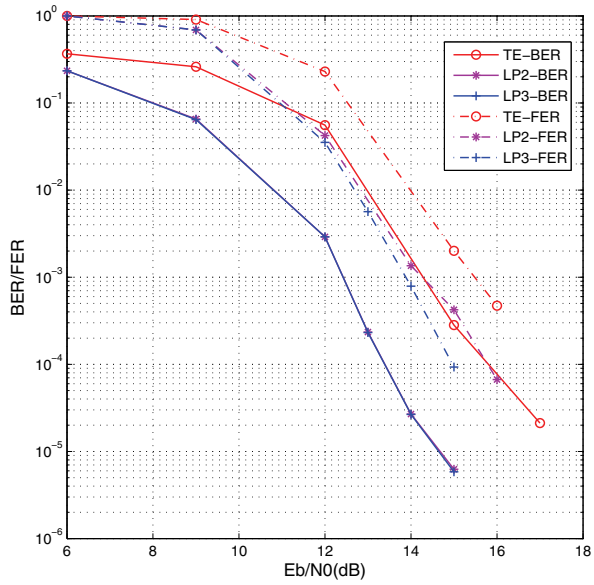

Fig. 10. BER (solid lines) and FER (dot-dashed lines) performance comparison of LDPC coded MIMO-OFDM systems with code C_2, 16QAM modulation, 2 transmit and 2 receive antennas.

10^{-4}. However, **LP3** still performs very well and is about 3.0 dB better than TE.

We also experiment with the case frequency selective channels has 5 random fading taps. The performance advantages of **LP2** and **LP3** over TE are similar to that of the preceding 3-tap channels.

D. High dimensional nonaffine QAM mapping

Recall that our proposed joint detection receivers are directly applicable to higher order modulation (e.g. 16QAM) with little modification. In particular, Gray-coded QAM mapping does not admit an affine relationship between the symbols

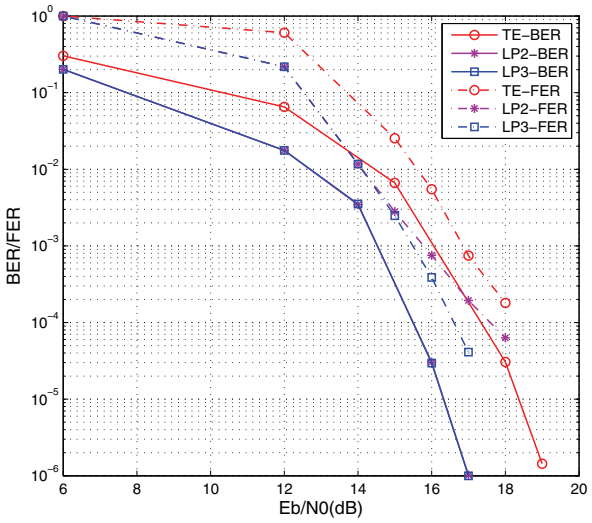

Fig. 11. BER (solid lines) and FER (dot-dashed lines) performance comparison of LDPC coded MIMO-OFDM systems with code C_3, 16QAM modulation, 2 transmit and 2 receive antennas.

and the bits, rendering the previous proposed LP1 receiver (based on affine QAM mapping) non-applicable. Our new detection algorithms overcome this obstacle.

We present the results from testing the 2×2 MIMO-OFDM systems in Fig. 10 and Fig. 11 under the 2 different LDPC codes, respectively. Note that the LDPC codes C_2 and C_3 are used in conjunction with Gray-coded 16QAM modulation. Since **LP1** is not applicable, our new receivers are tested and compared only against the turbo equalization (TE) receiver.

As shown in Fig. 10, the new joint detector **LP2** delivers nearly 3.0 dB gain compared with the TE at BER of 2×10^{-5}. Also, **LP3** performs as well as **LP2** in terms of BER, but achieves an advantage of 0.7 dB and 1.8 dB over **LP2** and TE, respectively, at FER of 5×10^{-4}. The performance gap between **LP3** and **LP2** will become wider at higher SNR. Fig. 11 illustrates the system performance when a higher rate code is used. From Fig. 11, we see that **LP2** works as well as **LP3** in terms of BER. However, both **LP2** and TE exhibit some "error-floor" effect at high SNR from the FER perspective. Nevertheless, our **LP3** performs more than 2.0 dB better than the traditional TE decoder at FER $\leq 1 \times 10^{-4}$.

E. Complexity Considerations

It is challenging to fully characterize the complexity of our joint detectors in terms of the number of addition and multiplication because simplex method is very efficient in practice but has an exponential worst case complexity. Hence, we investigate the relative complexity of our proposed joint detectors in terms of the average number of iterations, and the average size of constituent LP problems. All statistical data were obtained from simulations of the 4×4 MIMO system with code C_2 and three-tap multipath channel model. We ran our simulations repeatedly until 20 erroneous codewords were collected.

Fig. 12(a) compares the average number of iterations needed; that is, the average number of LP problems solved, to decode one codeword. Fig. 12(b) shows the average number of

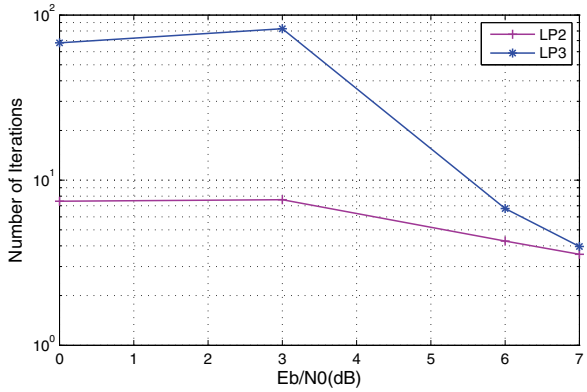

(a) Average number of iterations

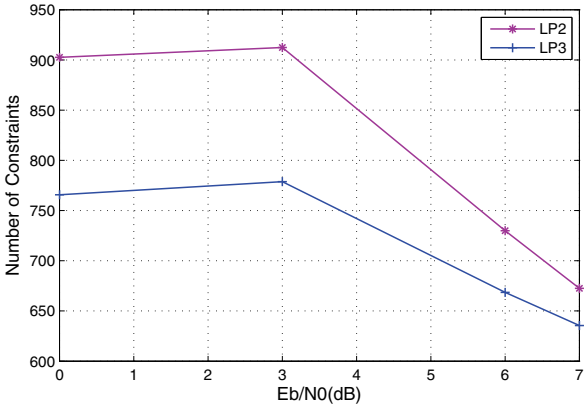

(b) Average number of constraints in final iteration

Fig. 12. Average number of iterations and Average number of constraints in final iteration for decoding one codeword.

constraints of the last LP problem in the iteration process that either generated a valid codeword or found a pseudo-codeword with no more cuts. In the first iteration, both LP2 and LP3 have $n + KN = 576$ constraints. At high SNR, such as SNR = 7 dB, LP2 and LP3 only need at most 4 iterations, and the number of constraints in the LP problem of the final iteration is under 700. Therefore, LP3 provides the much better FER performance than LP2 with the similar complexity in high SNR regime.

F. Summary

Our simulation tests considered different LDPC code rates, lengths, as well as various MIMO configures. From our extensive tests, We have demonstrated that the newly proposed joint receivers **LP2** and **LP3** provide substantial performance gains when compared with **LP1** both in terms of BER and FER. Our joint receivers also outperform the classic TE even if more turbo iterations and local iterations are used. The same conclusions are true for different number of multipath channel taps. Moreover, for under-determined MIMO systems (when there are more transmit antennas than receive antennas) or for high rate code (C_3), **LP2** tends to exhibit an error floor at very high SNR because of lower system redundancy or diversity. Nevertheless, **LP3** always exhibits outstanding FER performance in our tests. In particular, it always outperforms **LP2** in terms of FER, despite similar BER performance.

This performance gain is at the expense of somewhat higher complexity.

On the other hand, when considering BER, **LP2** works as well as **LP3** in most cases. Given the lower complexity of **LP2**, it is a suitable alternative for those systems in which low BER is more critical.

V. Conclusion

In this paper, we proposed a new linear-programming based receiver for the joint detection and decoding of LDPC-coded MIMO-OFDM systems. Unlike traditional disjoint serial detection-decoding receivers and other existing joint detection and decoding receivers based on belief propagation, our new joint receiver optimizes a unified global objective function to minimize the MIMO-OFDM detection error while simultaneously satisfying a number of linear constraints that are derived from the LDPC parity matrix. This single integrated optimization algorithm does not rely on blind mutual trust in message passing. Our receiver integrates the MIMO-OFDM signal detection and the decoding of LDPC coded data by solving a linear programming problem for practical QAM mappings. Our proposed joint MIMO-OFDM detector and decoder achieves substantial performance gain over existing joint detection receivers with comparable computational complexity.

Acknowledgment

The authors thank the Editor and the anonymous reviewers for devoting valuable time and effort in reviewing our manuscript.

References

[1] G. J. Foschini and M. J. Gans, "On limits of wireless communication in a fading environment when using multiple antennas," *Wireless Pers. Commun.*, vol. 6, pp. 311–335, 1998.

[2] J. H. Winters, J. Salz, and R. D. Gitlin, "The impact of antenna diversity on the capacity of wireless communication systems," *IEEE Trans. Commun.*, vol. 42, pp. 1740–1751, Feb./Mar./Apr. 1994.

[3] L. Cimini, "Analysis and simulation of a digital mobile channel using orthogonal frequency division multiplexing," *IEEE Trans. Commun.*, July 1985, pp. 665-675.

[4] G. L. Stuber, J. R. Barry, S. W. McLaughlin, Ye Li, M. A. Ingram, and T. G. Pratt, "Broadband MIMO-OFDM wireless communications," *Proc. IEEE*, vol. 92, no. 2, pp. 271–294, Feb. 2004

[5] M. Jiang and L. Hanzo, "Multiuser MIMO-OFDM for next-generation wireless systems," *Proc. IEEE*, vol. 95, no. 7, July 2007.

[6] H.-N. Lee, "LDPC coded modulation MIMO OFDM transceiver: performance comparison with MAP equalization," in *Proc. 2003 VTC – Spring*, vol. 2, pp. 1178–1182.

[7] B. Lu, G. Yue, and X. Wang, "Performance analysis and design optimization of LDPC coded MIMO OFDM systems," *IEEE Trans. Signal Process.*, vol. 52, no. 2, pp. 348–361, Nov. 2004.

[8] M. Sellathurai and S. Haykin, "Turbo-BLAST for wireless communications: theory and experiments," *IEEE Trans. Signal Process.*, vol. 50, no. 10, pp. 2538–2546, Oct. 2002.

[9] Part 11: Wireless LAN Medium Access Control (MAC) and Physical Layer (PHY) Specifications: High-Speed Physical Layer in the 5 GHz Band, IEEE Standard 802.11a-1999.

[10] Local and Metropolitan Area Networks-Part 16, Air Interface for Fixed Broadband Wireless Access Systems, IEEE Standard IEEE 802.16a.

[11] 3rd Generation Partnership Project (3GPP). (2009, Sep.) Evolved Universal Terrestrial Radio Access (E-UTRA); Physical channels and modulation. Available: http://www.3gpp.org/ftp/Specs/html-info/36211.htm.

[12] R. G. Gallager, "Low-density parity-check codes," *IRE Trans. Inf. Theory*, vol. 8, pp. 21–28, Jan. 1962.

[13] D. J. C. MacKay and R. M. Neal, "Good error-correcting codes based on very sparse matrices," *IEEE Trans. Inf. Theory*, vol. 45, no. 2, pp. 399–431, Mar. 1999.

[14] T. J. Richardson and R. Urbanke, "The capacity of low-density parity-check codes under message-passing decoding," *IEEE Trans. Inf. Theory*, vol. 47, pp. 599–618, Feb. 2001.

[15] X. Wang and H. V. Poor, "Iterative (Turbo) soft interference cancellation and decoding for coded CDMA," *IEEE Trans. Commun.*, vol. 47, pp. 1046–1061, July 1999.

[16] J. Feldman, M. Wainwright, and D. Karger, "Using linear programming to decode binary linear codes," *IEEE Trans. Inf. Theory*, vol. 51, no. 3, pp. 954–972, Mar. 2005.

[17] M. H. Taghavi and P. H. Siegel, "Adaptive methods for linear programming decoding," *IEEE Trans. Inf. Theory*, vol. 54, no. 12, pp. 5396–5410, Dec. 2008.

[18] A. Tanatmis, S. Ruzika, H. W. Hamacher, M. Punekar, F. Kienle, and N. Wehn, "A separation algorithm for improved LP-decoding of linear block codes," *IEEE Trans. Inf. Theory*, vol. 56, no. 7, pp. 3277–3289, Jul. 2010.

[19] X. Zhang and P. H. Siegel, "Adaptive cut generation algorithm for improved linear programming decoding of binary linear codes," *IEEE Trans. Inf. Theory*, vol. 58, no. 10, pp. 6581–6594, Oct. 2012.

[20] T. Cui, T. Ho, and C. Tellambura, "Linear programming detection and decoding for MIMO systems," in *Proc. 2006 IEEE ISIT*, pp. 1783–1787.

[21] M. H. Taghavi and P. H. Siegel, "Graph-based decoding in the presence of ISI," *IEEE Trans. Inf. Theory*, vol. 57, no. 4, pp. 2188–2202, Apr. 2011.

[22] M. F. Flanagan, "A unified framework for linear-programming based communication receivers," *IEEE Trans. Commun.*, vol. 59, no. 12, pp. 3375–3387, Dec. 2011.

[23] Y. Li, L. Wang, and Z. Ding, "Linear programming based joint detection of LDPC coded MIMO system," in *Proc. 2012 IEEE GLOBECOM*, pp. 4259–4264.

[24] T. Cui and C. Tellambura, "An efficient generalized sphere decoder for rank-deficient MIMO systems," *IEEE Commun. Lett.*, vol. 9, no. 5, pp. 423–425, May 2005.

[25] J.-L. Kim, U. N. Peled, I. Perepelitsa, V. Pless, and S. Friedland, "Explicit construction of families of LDPC codes with no 4-cycles," *IEEE Trans. Inf. Theory*, vol. 50, no. 10, pp. 2378–2388, Oct. 2004.

[26] H. Wymeersch, H. Steendam, and M. Moeneclaey, "Log-domain decoding of LDPC codes over GF(q)," in *Proc. 2004 IEEE ICC*,, pp. 772–776.

[27] C. Berrou and A. Glavieux, "Near optimum error correcting coding and decoding: Turbo-codes," *IEEE Trans. Commun.*, vol. 44, no. 10, pp. 1261–1271, Oct. 1996.

[28] J. Lodge, R. Young, P. Hoeher, and J. Hegenauer, "Separable MAP "filters" for the decoding of product and concatenated codes," in *Proc. 1993 IEEE ICC*,, pp. 1740–1745.

[29] M. C. Reed, C. B. Schlegel, P. D. Alexander, and J. A. Asenstorfer, "Iterative multiuser detection for CDMA with FEC: near-single-user performance," *IEEE Trans. Commun.*, vol. 46, no. 12, pp. 1693–1699, Dec. 1998.

[30] GNU Linear Programming Kit. Available: http://www.gnu.org/ software/glpk

[31] X.-Y. Hu, E. Eleftheriou, D. M. Arnold, and A. Dholakia, "Efficient implementations of the sum-product algorithm for decoding LDPC codes," in *Proc. 2001 IEEE GLOBECOM*.

Yong Li (S'11–M'13) Yong Li received the B.Sc. degree in Electronic and Information Engineering from Chongqing University of Posts and Telecommunications (CQUPT), Chongqing, China, in 2003, the M.S. degree and the Ph.D degree in Communication Engineering from Xiamen University, Fujian, China, in 2006 and 2012, respectively. From Jan. 2013, he joined CQUPT, where he is currently an assistant Professor in the Key Lab of Mobile Communication. From Sep. 2006 to Jan. 2007, he was a research assistant in the department of Electronic Engineering, City University of Hong Kong. From Feb. 2007 to Aug. 2009, he was with Gallop Inc., Chongqing, China. From Sep. 2011 to Aug. 2012, he visited University of California, Davis, USA, as a visiting scholar. His primary research interests include channel coding, MIMO-OFDM, joint blind equalization and decoding. .

Lin Wang (S'99–M'03–SM'09) received the B.Sc. degree in Mathematics with first class honors) from the Chongqing Normal University, Chongqing, China, in 1984, the M.Sc. degree in Applied Mathematics from the Kunming University of Technology, Kunming, China, in 1988, and the Ph.D. degree in Electronics Engineering from the University of Electronic Science and Technology of China, Chengdu, China, in 2001.

He has become Distinguished Professor since 2012 in Department of Communication Engineering in School of Information Science and Technology of Xiamen University, China, where he joined as a professor since 2002. He was with the Center of Chaos and Complexity Network in Department of Electronics Engineering of City University of Hong Kong as one visiting researcher during Jan. to April of 2003 and with Department of Electrical and Computer Engineering in University of California at Davis as Senior Research Scholar during Jan. to July of 2013. He had been supported as New Century Excellent Talents (NCET) by Administration Education of China in 2004 and obtained Bendong Sa Chair Professor Award of Xiamen University in 2012. His researching field includes Wideband Wireless Communication Theory (Cross-layer Design, Adaptive transmissionCooperative Communication, UWB Based on Chaotic Modulations), Information Theory (Source coding, Channel coding, joint source and channel encoder and decoder, Network Coding) and their applications. He has published over 80 refereed journal and conference papers and owned 8 Chinese Patents. Meanwhile he is also the senior member of IEEE, associate editor of Acta Electronica Sinica from 2011 to 2015, and Guest Associate Editor of International Journal of Bifurcations and Chaos (IJBC) from 2010 to 2011. He had also organized IEEE ICCCAS 2008 and IEEE NAS 2012 as Co-Chairs of Technical Program Committee and Co-General Chairs respectively. .

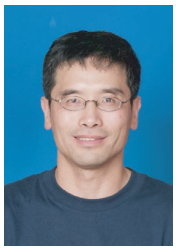

Zhi Ding (S'88-M'90-SM'95-F'03) is the Child Family Endowed Professor of Engineering and Entrepreneurship at the University of California, Davis. He also holds a joint appointment as a thousand-talent professorship at Southeast University in Nanjing, China. He received his Ph.D. degree in Electrical Engineering from Cornell University in 1990. From 1990 to 2000, he was a faculty member of Auburn University and later, University of Iowa. Prof. Ding has held visiting positions in Australian National University, Hong Kong University of Science and Technology, NASA Lewis Research Center and USAF Wright Laboratory. Prof. Ding has active collaboration with researchers from several countries including Australia, China, Japan, Canada, Taiwan, Korea, Singapore, and Hong Kong.

Dr. Ding is a Fellow of IEEE and has been an active member of IEEE, serving on technical programs of several workshops and conferences. He was associate editor for IEEE TRANSACTIONS ON SIGNAL PROCESSING from 1994-1997, 2001-2004, and associate editor of IEEE SIGNAL PROCESSING LETTERS 2002-2005. He was a member of technical committee on Statistical Signal and Array Processing and member of technical committee on Signal Processing for Communications (1994-2003). Dr. Ding was the Technical Program Chair of the 2006 IEEE Globecom. He is also an IEEE Distinguished Lecturer (Circuits and Systems Society, 2004-06, Communications Society, 2008-09). He served on as IEEE TRANSACTIONS ON WIRELESS COMMUNICATIONS Steering Committee Member (2007-2009) and its Chair (2009-2010). Dr. Ding received the 2012 IEEE Wireless Communication Recognition Award from the IEEE Communications Society and is a coauthor of the text: *Modern Digital and Analog Communication Systems*, 4th edition, Oxford University Press, 2009.